Deep-Sea Research II 55 (2008) 2106–2117

Contents lists available at ScienceDirect

Deep-Sea Research II

journal homepage: www.elsevier.com/locate/dsr2

Variability on phytoplankton size structure in the western Antarctic Peninsula (1997–2006)

M.A. Montes-Hugo [a,*], M. Vernet [a], D. Martinson [b], R. Smith [c], R. Iannuzzi [b]

[a] Scripps Institution of Oceanography, University of California, San Diego, La Jolla, CA 92093-0218, USA
[b] Lamont-Doherty Earth Observatory of Columbia University Palisades, NY 10964, USA
[c] Department of Geography, University of California, Santa Barbara, Santa Barbara, CA 93106, USA

ARTICLE INFO

Article history:
Accepted 30 April 2008

Keywords:
Phytoplankton size structure
Satellite sensing
Time series
Polar waters
Sea ice
Size distribution

ABSTRACT

The temporal and spatial variability of phytoplankton size structure of waters west of the Antarctica Peninsula (WAP) was investigated between 1997 and 2006. Time series of satellite-derived (phytoplankton size structure index or $\gamma_{b_{bp}}$, chlorophyll *a* concentration or chl_T, and sea-ice extent) and shipboard (temperature, salinity, nutrients, and mixed-layer depth) variables were generated during spring–summer in slope, middle shelf and inshore waters and analyzed in relation to atmospheric anomalies (El Niño Southern Oscillation, ENSO, and Southern Annular Mode, SAM). The sampling design included stations north (northern, 62°S) and within (central and southern, 64–68°S) the Pal-LTER (Palmer Long Term Ecological Research) study site. It is hypothesized that contribution of 'small' phytoplankton (<20 μm) has increased in the last decade in WAP waters due the ongoing regional climate change. Relationships between $\gamma_{b_{bp}}$, the spectral slope of particle backscattering, and environmental parameters were explored based on non-parametric trends (Mann–Kendall test) and cross-correlation coefficients (Spearman matrix). Three types of temporal patterns were detected in satellite-derived phytoplankton size distributions: (1) inter-annual variations of spring–summer $\gamma_{b_{bp}}$ related to monthly sea-ice extent, (2) abrupt transitions toward dominance of 'small' (<20 μm) phytoplankton cells (high $\gamma_{b_{bp}}$) and low chl_T values (<1 mg m^{-3}) during 1998 and 2003 summer seasons, and (3) positive or negative trends (decrease vs increase of mean cell size) in specific domains of central and northern stations. Temporal transitions in cell size coincided with a switch on ENSO and SAM anomalies as well as increase of heat content of shelf waters over the WAP region. The lack of offshore spring bloom and summer shelf bloom most likely explains the dominance of relative small phytoplankton cells during the 1998 and 2003 summer seasons. A greater frequency of southerly winds during spring and autumn is expected to favor the dominance of 'small' (<20 μm) phytoplankton cells over WAP waters. Conversely, the greater intensification of the Antarctic Circumpolar Current interaction with the WAP shelf-break during SAM+ years is expected to intensify topographically induced upwelling and favor the dominance of 'large' (>20 μm) phytoplankton cells on slope waters of central stations. The well-described 50-year warming trend in the Antarctic Peninsula has not resulted in a consistent trend in phytoplankton size structure, as originally hypothesized, but a mosaic of trends attributed to anomalous mesoscale changes of sea-ice extent and circulation patterns.

1. Introduction

The western shelf of the Antarctic Peninsula (WAP) is one of marine regions in the world that might be more vulnerable to global climate change due to a relative shallow water column, a wider continental shelf, and a strong ice influence (Smith et al., 1995; Smith and Stammerjohn, 2001; Martinson et al., 2008). In the last few decades, variability in macro-zooplankton (e.g., increase of frequency of salp blooms; Loeb et al., 1997; Perissinotto and Pakhomov, 1998; Ross et al., 2008) and top predators (e.g., decline of Adelie penguin populations; Fraser and Patterson, 1997) of the WAP region has been linked to climate effects (e.g., sea-ice extent, shift of ocean heat flux). These studies also suggested that part of the observed trends might be attributed to modifications of food-webs pathways and concomitant modifications on food size spectra and composition. In the WAP region, food transference between phytoplankton and zooplankton follows two general models according to the size distribution of phytoplankton assemblages (Walsh et al., 2001):

* Corresponding author at: 71 Dudley Road, New Brunswick, NJ 08901-8521, USA. Tel.: +1 732 9326555; fax: +1 732 9328578.
E-mail address: montes@marine.rutgers.edu (M.A. Montes-Hugo).

0967-0645/$ - see front matter © 2008 Published by Elsevier Ltd.
doi:10.1016/j.dsr2.2008.04.036

pico-nanophytoplankton (<20 μm, cryptophytes and unicellular *Phaeocystis antarctica*), microphagous zooplankton (salps and small copepods), and microphytoplankton (>20 μm, 'large' diatoms) crustacean zooplankton (krill and large copepods).

On the basis of *in situ* evidence, the rapid atmospheric warming of the WAP region between 1950 and 2005 (up to 6.5 °C increase during July) coincides with increased heat advection caused by winds blowing from lower latitudes (northerly) and intrusion of warmer waters (upper layer of Antarctic Circumpolar Current or ACC) onto the WAP shelf (Martinson et al., 2008; Stammerjohn et al., 2008). The intensification of northerly winds and ACC intrusions responds to stronger La Niña events and positive values of SAM (Southern Annular Mode). This climate variability translates in sea-ice decrease (earlier retreat) and is expected to affect size distribution of phytoplankton community either through the timing of phytoplankton development or dominance of 'small' (<20 μm) vs 'large' (>20 μm) cells.

A greater dominance of 'small' phytoplankton (e.g., cryptophytes) over 'large' phytoplankton (e.g., diatoms) communities in coastal WAP waters has been hypothesized as a response to the regional warming (Moline et al., 2004). However, lack of field data has restricted a rigorous testing. Evidence is also lacking regarding which factors (bottom-up vs top-down) modulate variations on phytoplankton size structure of the WAP ecosystem within the time frame of >5 and <30 years. For Antarctic waters, Smith and Lancelot (2004) proposed that bottom-up (e.g., sea-ice dynamics) factors mainly control the growth of 'large' phytoplankton cells, while top-down (e.g., microzooplankton grazing) environmental forcing will preferentially control communities dominated by 'small' phytoplankton cells. This hypothesis is consistent with the preferential growth of larger diatoms along the Antarctic Polar Front due to the greater micronutrient (e.g., iron) supply (bottom-up mechanism; De Baar et al., 1997), and lower abundance of 'small' cells due to enhanced microzooplankton grazing (Landry et al., 2001). However, Smith and Lancelot's hypothesis is too simplistic to explain other mechanisms where 'small' (<20 μm) phytoplankton cells (e.g., *P. antarctica*) are favored by micronutrients such iron (Sedwick et al., 2007) or are almost unaffected by microzooplankton grazing (top-down; Caron et al., 2000).

Recently, Montes-Hugo et al. (2008) proposed the use of satellite-derived observations to estimate phytoplankton size characteristics over WAP waters. This novel technique is a promising tool to extend field measurements on the shelf through the growth season (November to February), allowing mapping of large areas in a synoptic way. Remoteness and extreme weather conditions make *in situ* characterization of Southern Ocean waters a challenging task. For this reason, the description of phytoplankton community characteristics, including size structure distributions, over the WAP region has not been systematic (Bidigare et al., 1996; Rodriguez et al., 2002) or representative at a regional scale (Holm-Hansen et al., 1989; Prézelin et al., 2004). Summer observations (January) evidence short-term periodicities (e.g., replacement of diatoms by flagellates during seasonal succession; Moline and Prézelin, 1996; Moline et al., 1997; Garibotti et al., 2003a) and different phytoplankton assemblages over the WAP shelf. For example, a community dominated by large diatoms-cryptomonads (*Pyramimonas*) was observed in waters surrounding Anvers Island and a community of large diatoms (*Phaeocystis-Pyramimonas*) was most abundant in Marguerite Bay, as previously observed in Gerlache Strait (Varela et al., 2002; Garibotti et al., 2003b, 2005a, b). These studies could distinguish important environmental factors affecting timing (e.g., sea-ice retreat) and spatial distribution (e.g., shelf-break influence, upper mixed-layer variability) of phytoplankton communities over the WAP. However, none of these studies addressed time scales longer than a few (<5) years or quasi-simultaneous comparisons ('snapshots') of phytoplankton communities of northern and southern WAP shelf.

The objective of this study is to explore changes (within one decade, 1997–2006) on phytoplankton size structure in the WAP region and its relationship with the ongoing regional climate trends. Phytoplankton size distributions were estimated from satellite-derived spectral slope of particle backscattering ($\gamma_{b_{bp}}$), a bulk optical property that varies inversely with the mean diameter of particles. The final goal is to elucidate phytoplankton variability in the context of large-scale ecosystem variability influenced by sea-ice fluctuations and by a latitudinal climate migration (Smith and Stammerjohn, 2001, 2003). Since years with an early sea-ice retreat favor presence of small flagellates over diatoms during summer, Garibotti et al. (2005a) suggested that summer seasons of warm years (shorter ice season) should be dominated by a complex food chain where primary producers are mainly represented by 'small' phytoplankton (nanophytoplankton). Therefore and consistent with the sustained warming over the WAP area since 1950, it is hypothesized that contribution of 'small' phytoplankton (<20 μm) has been increased in the last decade in WAP waters due the ongoing regional climate change.

To test this hypothesis, *in situ* information was gathered between 1997 and 2006 as part of the Palmer Station-Long term Ecological Research (Pal-LTER; Smith et al., 1995). Inter-annual variability of phytoplankton size structure was estimated with field measurements (size-fractions of chlorophyll *a* concentration) and a remote-sensing index based on particle size distributions (Montes-Hugo et al., 2008). The index was calculated from satellite imagery and related to temporal trends of meteorological (anomalies of sea-ice extent, ENSO or El Niño Southern Oscillation, and SAM), hydrological (temperature, salinity, mixed-layer depth (MLD) and macronutrients), and biological (total or chl_T and >20 μm or $chl_{(>20\,\mu m)}$ chlorophyll *a* concentrations) parameters.

2. Methods

2.1. Shipboard environmental measurements

Oceanographic surveys over the WAP region were carried out every austral summer (January–February) between 1997 and 2006 as part of the Pal-LTER program. The sampling grid (~250 km cross-shelf × 500 km along-shelf, grid lines 200–600, Fig. 1, Waters and Smith, 1992) was covered in ~28 days, overlying a broad continental shelf averaging ~400 m in depth.

Bathymetry and hydrographic conditions divide Pal-LTER grid into three domains (Fig. 1; Waters and Smith, 1992; Smith et al., 1995; Martinson et al., 2008): coastal or inshore (stations 0–60), shelf (stations 80–120), and continental slope (stations 140–200). Summer cruises encompass transects 200–600 of Pal-LTER grid (hereafter WAP sampling grid) even though transects 0–900 were originally proposed when the LTER site was created (Waters and Smith, 1992; Fig. 1). Across a latitudinal gradient, grid lines (GD) 200 (68°S), 600 (64°S) and 900 (62°S) represent contrasting different average sea-ice conditions (e.g., ~25 more days with ice in GD 200 than in GD 600 from 1978 to 2004; Stammerjohn et al., 2008).

For each sub-region (one domain along grid line), the monthly average and standard error of each *in situ* parameter was calculated. Time series for water temperature, salinity, MLD and nutrient concentrations, and total chlorophyll *a* or chl_T were generated for 1997–2005, respectively. All data (up to 17,400 per variable) are available in the Pal-LTER database (http://pal.lternet.edu/data/).

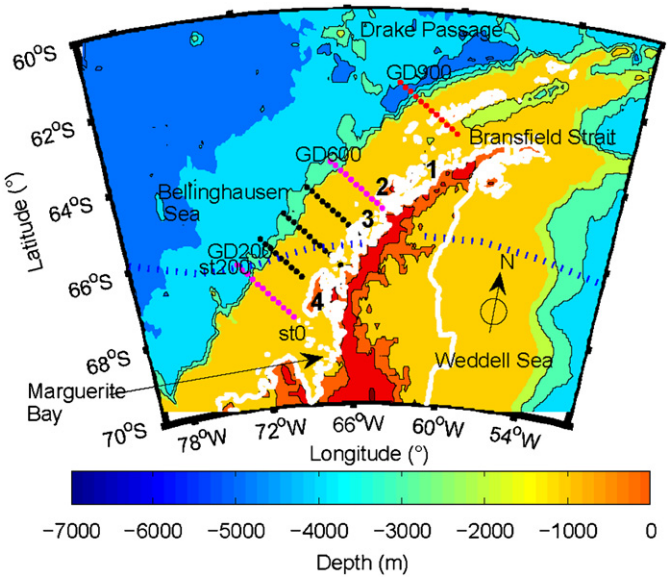

Fig. 1. Map of the study area. Geographic points are represented using a conic Lambert projection. Sampling grid over WAP (west shelf of the Antarctica Peninsula) waters (solid circles). Time series were generated on grid lines (GD) 200 (southern) and 600 (central) of Pal-LTER sampling grid (solid pink dots), and 900 (northern transect, solid red circles). Coastal or inshore (stations 0–60), shelf (stations 80–120), and continental slope (stations 140–200) sampling locations (st) are situated every 20 km apart along the shelf. All grid lines (lines 200–900) are spaced every 100 km from north to south and run perpendicular to the average coastline: (1) Bransfield Strait, (2) Anvers Island, (3) Renaud Island, (4) Adelaide Island. Medium resolution coastline data (1:75,000) was obtained from NOAA/NOS coastline extractor website and includes the perennial sea-ice edge (http://rimmer.ngdc.noaa.gov/mgg/coast/getcoast.html) (continuous white line). Seasonal sea-ice extent is indicated for an average year (summer 1997) (National Snow and Ice Data Center is shown; Smith and Stammerjohn, 2001) (dashed blue line). Bathymetric contours were constructed with a 5-min (~8 km) topographic dataset with isobaths every 1 km (TerrainBase, National Geophysical Data Center).

In general for all in-water variables, samples were collected at the depth corresponding to the 50% of incident radiation at the sea surface, well above the detection depth (~2.5–19 m) of ocean-color sensors (Montes-Hugo et al., 2008). Samples for chl_T and $chl_{(>20\,\mu m)}$ were obtained after filtration of 125–250 ml of seawater through 0.45-μm nominal pore size (mixed cellulose acetate and nitrate, Millipore, HAWP) and 20-μm (Nylon mesh) filters, respectively. chl_T and $chl_{(>20\,\mu m)}$ measurements (in mg m^{-3}) were analyzed by fluorometry (Smith et al., 1981). Fraction of $chl_{(>20\,\mu m)}$ with respect to the non-fractioned sample ($chl_{(>20\,\mu m)}/chl_T$) was calculated for the same light level.

Surface-water temperature and salinity measurements were conducted during the 1997 cruise with a Seabird SEACAT system integrated into the Bio-optical Profiling System (BOPS; Smith et al., 1997), and since 1998 (and deep stations of 1997) with a standard CTD (SeaBird 911+CTD system; Martinson et al., 1999). Mixed-MLD was calculated as the local maxima in the second derivative of the density profile according to Martinson and Iannuzzi (1998).

Samples for nutrient concentrations (NO_3^-+NO_2^-, NH_4^+, PO_4^{3-}, and H_4SiO_4) were obtained with Niskin or Go Flo bottles (5 or 10 l), and aliquots were sampled in polypropylene bottles (20–30 ml) previously washed with diluted HCl (10%). Chemical determinations were made aboard the ship with an Alpkem System or frozen and analyzed at the Marine Science Analytical Laboratories, University of California, Santa Barbara (1999) using continuous flow injection (Johnson et al., 1985). Monthly averages of 0–10 m sea surface temperature, salinity and nutrient concentrations were calculated for each year.

2.2. Satellite imagery products

2.2.1. Phytoplankton size structure index

Since particle size distributions covary with phytoplankton size structure over WAP waters, an optical parameter sensitive to particle size-spectra ($\gamma_{b_{bp}}$; Gordon and Morel, 1983) was estimated using satellite observations to derive contribution of 'large' vs 'small' phytoplankton cells (Montes-Hugo et al., 2008):

$$\gamma_{b_{bp}} = Y0 + Y1\frac{R_{rs}(443)}{R_{rs}(488)}, \quad (1)$$

where $\gamma_{b_{bp}}$ is the spectral slope of particle backscattering that increases as particles become smaller, $Y0 = -1.13$, $Y1 = 2.57$, determination coefficient (r^2) = 0.59 (Carder et al., 2004).

Remote-sensing reflectance (R_{rs}) is calculated from satellite imagery (Montes-Hugo et al., 2005) provided by SeaWiFS (Sea-viewing Wide Field-of-view Sensor). On the basis of data collected in WAP waters, Montes-Hugo et al. (2008) found an inverse functionality between $\gamma_{b_{bp}}$ and biomass contribution of large phytoplankton cells (>20 μm):

$$\gamma_{b_{bp}} = \frac{-[\log\{(chl_{(>20\,\mu m)}/chl_T)/A)\}]}{B}; \quad r^2 = 0{:}85, \quad (2)$$

where $A = 8.892$ and $B = -0.8189$ with uncertainties (1 S.E.) of 1.517 and 0.108, respectively. The use of phytoplankton biomass spectra (specifically the slope of the log-distribution) to estimate different cell size distributions of phytoplankton is not novel in the literature (Sprules and Munawar, 1986). Further details regarding the empirical algorithm of $\gamma_{b_{bp}}$ and $\gamma_{b_{bp}} - chl_{(>20\,\mu m)}/chl_T$ relationship can be examined in Carder et al. (1999) and Montes-Hugo et al. (2008), respectively. In the WAP region, the performance of $\gamma_{b_{bp}}$ model (2) to detect phytoplankton assemblages with dominance of 'large' vs 'small' cells is ~80%.

Global area coverage (GAC) images with 4.5 km spatial resolution were obtained from SeaWiFS (http://oceancolor.gsfc.nasa.gov/, NASA) between November 1997 and February 2006. L2 imagery products were collected between 60°S 80°W and 70°S 50°W; thus, satellite scenes covered coastal and oceanic domains of the WAP sampling grid (Fig. 1). Only those swaths containing a minimum of 25% pixels with geophysical units were chosen. To remove multiple-scattering effects (sun zenith angle greater than 50°) on atmospheric correction (Gordon et al., 1988), only images between November 1 and February 8 of each season were analyzed.

The Windows Image Manager (WIM) software (http://www.wimsoft.com/) was used to read the R_{rs} values from L2 imagery (HDF format). Low-quality pixels were removed from L2 datasets using level-3 flags. SeaWiFS-derived $\gamma_{b_{bp}}$ values were computed with customized software written using the Microsoft NET framework. The WIM automation module (WAM) software was applied to generate time series of $\gamma_{b_{bp}}$ for different regions along and across the WAP shelf. Additional time series were produced farther north of the summer LTER sampling grid and across the Bransfield Strait (line 900, Fig. 1) to extend the sampling from 62°S to 68°S.

In describing the spatial and temporal patterns, 'northern', 'central' and 'southern' stations refer to those sampling locations along grid lines 900, 600, and 200, respectively. For each sub-region, the monthly average and standard error of pixels with valid $\gamma_{b_{bp}}$ values ($\gamma_{b_{bp}}$ between 0.8 and 3.0) were computed with a mask of 2 × 2. Given the number of pixels per sub-region, the average was comparable with the median (i.e., a descriptor less influenced by outliers). According to Montes-Hugo et al. (2008), a $\gamma_{b_{bp}}$ value of 1.668 was a fair predictor to differentiate WAP waters dominated by 'large' ($chl_{(>20\,\mu m)}/chl_T \geqslant 0.5$, $\gamma_{b_{bp}} \leqslant 1{:}668$) vs 'small' ($chl_{(>20\,\mu m)}/chl_T < 0.5$, $\gamma_{b_{bp}} > 1{:}668$) phytoplankton cells.

2.2.2. Chlorophyll a concentration

Time series of chl_T also were derived using $R_{rs}(490)/R_{rs}(555)$ ratios from SeaWiFS data (hereafter chl_{DS}; Dierssen and Smith, 2000). Chlorophyll estimates using the cubic polynomial empirical relationship of Dierssen and Smith (2000) differ by roughly a factor of 2 with respect to those estimates derived from the global standard ocean-color model (SeaWiFS OC-4; O'Reilly et al., 1998).

2.2.3. Sea-ice extent

Sea-ice concentration data were obtained from passive microwave satellite sensors (Scanning multi-channel microwave radiometer and special sensor microwave/imager, SMMR-SSM/I). Time series of sea-ice extent, ocean area enclosed by the 15% sea-ice concentration contour, were derived using the Goddard Space Flight Center (GSFC) Bootstrap passive microwave algorithm (Comiso, 1995). Monthly sea-ice extent is provided by EOS Distributed Archive Center (DAAC) at the National Snow and Ice Center (NSIDC), University of Colorado in Boulder, CO (http://nsidc.org). Sea-ice extent datasets (1978–2005) within the WAP region were obtained from Stammerjohn et al. (2003). Description of the sea-ice concentration algorithm is given by Comiso et al. (1997). SMMR-SSM/I imagery has a pixel size of approximately $25 \times 25\,km^2$ at nadir, and a temporal resolution of 1 day.

2.3. Statistical analysis

Non-parametric Mann–Kendall test (Mann, 1945; Kendall, 1975) was applied for detection of trends (increasing or decreasing magnitude within the study period) of *in situ* measurements and satellite estimates (ocean color and microwave). Monthly decomposition of trends was done according to a seasonal modified version (Hirsch et al., 1982). Detection of trends with different time windows is especially suitable in the WAP region since the occurrence of transient hydrographic phenomena (e.g., offshore/inshore migration of phytoplankton bloom development; Smith et al., 2008) that may alter local phytoplankton size structure dynamics. The univariate statistic (MK) for a time series $\{Z_k, k = 1,2,\ldots,n\}$ of data is defined:

$$MK = \sum_{j<1}^{j=n-1} \operatorname{sgn}(Z_i - Z_j), \tag{3}$$

where $\operatorname{sgn}(x) = 1$, if $x > 0$, 0 if $x = 0$, -1 if $x < 0$. A positive or negative value of MK (Sens slope) is indicative of increasing or decreasing trend. A macro written in excel was used to compute seasonal and non-seasonal trends (Libiseller and Grimvall, 2002).

Relationships between $\gamma_{b_{bp}}$ values and environmental variables were evaluated for each domain (inshore, middle shelf and slope) of each transect with Spearman rank correlation (Sokal and Rohlf, 1995). In line 900 (northern stations), correlations were only performed between $\gamma_{b_{bp}}$ and satellite-derived products (sea-ice extent and chl_{DS}) since we lack *in situ* measurements. The greater the differences between two sequences of ranked variables, the lower the Spearman correlation coefficient (R).

To evaluate how dependent was the phytoplankton size structure index on inter-annual variability of sea-ice extent and main atmospheric anomalies (ENSO or El Niño Southern Oscillation and SAM or Southern annular mode), R values were computed between summer $\gamma_{b_{bp}}$ and previous winter ENSO/SAM monthly anomalies (lag $= -1$ year). ENSO and SAM anomalies have a strong influence on sea-ice extent of the WAP region (Kwok and Comiso, 2002; Liu et al., 2004; Martinson et al., 2008; Stammerjohn et al., 2008). Also, a dependency between ENSO and SAM anomaly fluctuations can be expected for the study area (Simmonds and King, 2004; Stammerjohn et al., 2008).

The multivariate ENSO index (MEI) data were obtained from the National Oceanographic and Atmospheric administration (NOAA, Earth System Research Laboratory). MEI is the first unrotated principal component estimated from surface wind, sea-surface temperature and cloudiness fraction of the sky components (Wolter and Timlin, 1998). The SAM index used here is an observation-based index (Marshall, 2003) and is calculated as the difference of normalized monthly zonal mean sea-level pressure values (mean of six stations) estimated at 40° and 65°S.

Mann–Kendall test and Spearman correlation are particularly suitable in time series of the WAP region since these analyses are not sensitive to data discontinuity caused by meteorological conditions (e.g., clouds in ocean-color imagery) and lack of normality derived from non-linear processes.

3. Results

3.1. Phytoplankton size structure index

In general for the same month and due to time differences on sea-ice retreat advance between regions, more valid satellite-derived R_{rs} values (e.g., pixels without interference of sea-ice cover) were obtained in oceanic waters north of the WAP sampling grid than further South. Therefore, multiyear average of $\gamma_{b_{bp}}$ in slope waters of northern stations contained late spring to summer data (November–February) while average of inshore waters of southern stations was primarily computed with summer data (January–February). In general, the average of $\gamma_{b_{bp}}$ values between November and February and for the period 1997–2006 was significantly greater in slope (up to 1.997) than in inshore (up to 1.357) waters (Fig. 2). A large inter-annual variability of $\gamma_{b_{bp}}$ was observed toward offshore waters (up to7 0.067, 1 S.E.; Fig. 2B, E and H). Inshore waters of southern stations had the greatest proportion of pixels dominated by 'large cells' ($>20\,\mu m$) or $\gamma_{b_{bp}} \leqslant 1{:}668$ (up to 81.8%, Fig. 2F) while the opposite was true for slope waters of northern stations (up to 23.1%, Fig. 2B). Field data of chlorophyll *a* size fractions confirmed the presence of 'large' cells in inshore waters of the southern stations (Table 1).

A general monthly increase of $\gamma_{b_{bp}}$ (i.e., 'large particles' are removed) was observed in slope waters of WAP as the season progresses, albeit with difference in timing at different latitudes (Fig. 3). In contrast, inshore and middle shelf domains did not have a unique spring–summer variation of $\gamma_{b_{bp}}$ (e.g., Fig. 3A and B). In a longer time scale (1997–2006), a consistent increase of $\gamma_{b_{bp}}$ (higher contribution of smaller particles) was detected in inshore waters of northern stations during February (Mann–Kendall test, $MK = 2.227$, $P = 0.026$, Supplemental Table 1, Fig. 2A).[1] Conversely, a sustained drop of $\gamma_{b_{bp}}$ values ('large' particles are present) was observed for December in slope waters of central stations ($MK = -2.474$, $P = 0.013$, Supplemental Table 2, Figs. 2E and 3B).

Cyclic temporal patterns also were observed (Fig. 2). The most conspicuous shows two maxima in $\gamma_{b_{bp}}$ (greater contribution of smaller particles) on January 1998 and 2003 for slope waters in the South, followed by lower $\gamma_{b_{bp}}$ values in the subsequent seasons. This 5-year cycle was somewhat evident in other spatial domains across and along the WAP shelf region (Fig. 2A, B, D, G, H).

[1] Due to their size, Supplementary Tables 2–4 can be found at / http://pal.internet.edu/publications/deepseaS.

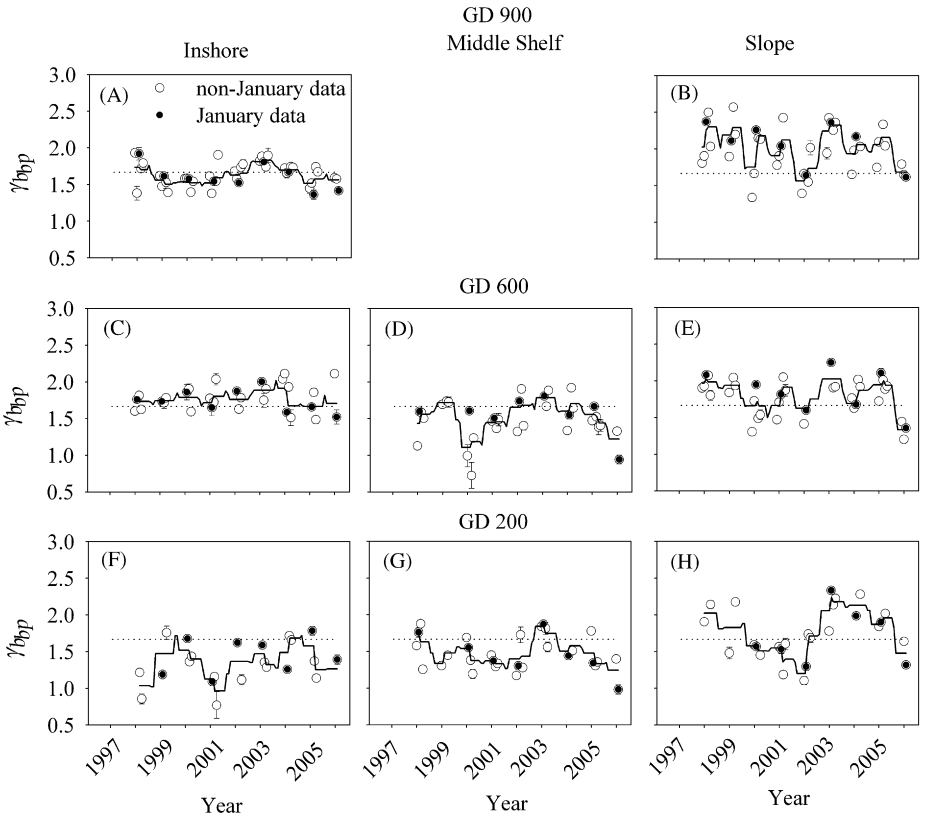

Fig. 2. Time series of spectral slope of particle backscattering ($\gamma_{b_{bp}}$) in the WAP region. For grid line (GD) 900 (northern transect, panels A and B), middle shelf data are not depicted because this domain is occupied by Livingston Island. GD 600 (panels C–E) and GD 200 (panels F–H) correspond to central and southern stations of WAP sampling grid, respectively. Threshold at which $chl_{(>20\,\mu m)}/chl_T = 0.5$ and $\gamma_{b_{bp}} \leqslant 1.668$ is symbolized (dotted line). Each point in the graph represents a monthly average (November to February) 7 1 S.E. No monthly values are plotted when data are of poor quality or significantly affected by clouds or sea ice.

Table 1
Average and standard error of phytoplankton size-structure parameters and ancillary data for WAP time series

	GD 900			GD 600			GD 200	
	I	Sl	I	M	Sl	I	M	Sl
$\gamma_{b_{bp}}$	1.61 (0.06)	2.07 (0.11)	1.74 (0.05)	1.55 (0.09)	1.85 (0.10)	1.45 (0.09)	1.45 (0.09)	1.70 (0.14)
chl_{DS}	0.97 (0.24)	0.13 (0.05)	2.48 (1.06)	1.59 (1.10)	0.42 (0.23)	3.34 (1.08)	2.29 (1.43)	0.32 (0.12)
$chl_{(>20\,\mu m)}/chl_T$			0.19 (0.10)	0.18 (0.13)	0.19 (0.10)	0.49 (0.11)	0.22 (0.15)	0.16 (0.06)
T			1.17 (0.33)	1.00 (0.25)	1.29 (0.20)	0.88 (0.25)	1.16 (0.15)	1.06 (0.27)
S			33.62 (0.06)	33.75 (0.08)	33.68 (0.07)	33.52 (0.09)	33.62 (0.06)	33.55 (0.12)
MLD			25.17 (5.23)	20.60 (4.95)	36.08 (6.14)	30.72 (4.98)	27.33 (22.67)	36.00 (5.24)
NIT			21.31 (0.17)	22.01 (0.17)	21.05 (0.22)	18.97 (0.24)	19.71 (0.19)	20.15 (0.24)
NH_4^+			1.43 (0.05)	1.67 (0.06)	1.31 (0.05)	1.22 (0.04)	1.51 (0.19)	1.45 (0.05)
PO_4^{3-}			1.50 (0.02)	1.56 (0.02)	1.41 (0.02)	1.44 (0.01)	1.32 (0.02)	1.33 (0.01)
H_4SiO_4			65.32 (0.54)	61.37 (1.05)	58.13 (0.64)	52.04 (1.02)	57.62 (0.29)	48.28 (0.76)

For 1997–2006, January measurements of satellite-derived spectral slope of particle backscattering ($\gamma_{b_{bp}}$) and total chlorophyll *a* concentration (chl_{DS}), and contribution of *in situ* chlorophyll *a* concentration >20 μm with respect to the total ($chl_{(>20\,\mu m)}/chl_T$) are indicated for inshore (I), middle shelf (M) and slope (Sl) waters. For seawater temperature (T), salinity (S) and mixed-layer depth (MLD) only 1997–2005 data were available. Grid line (GD) 900 has not middle shelf stations; chl_{DS} in mg m^{-3}, T in °C, S in psu, MLD in m, nitrate+nitrite (NIT), ammonia (NH_4^+), phosphate (PO_4^{3-}), and silicic acid (H_4SiO_4) concentrations in μM. Between parentheses is 1 S.E.

3.2. Phytoplankton biomass

As expected, oligotrophic waters ($chl_{DS} < 1$ mg m^{-3}; Garibotti et al., 2003a) were more common to the north and offshore of the WAP region. Highest satellite-derived chlorophyll *a* values were calculated in inshore waters of southern stations (up to 3.47 mg m^{-3}), while lowest values corresponded to the outermost region along the shelf break of northern stations (not higher than 0.26 mg m^{-3}, Fig. 4B and F). In contrast to $\gamma_{b_{bp}}$, the greatest interannual variability of chl_{DS} values was found in those stations nearest to the coast. In general, higher chl_{DS} values corresponded with lower $\gamma_{b_{bp}}$ values (Spearman correlation, $R = -0.42$ to -0.91, Supplementary Table 2; Figs. 2 and 4) but there were some exceptions. For instance, middle shelf chl_{DS} values of central stations were intermediate compared to those estimated in inshore and slope regions (Fig. 4C–E), albeit $\gamma_{b_{bp}}$ values were the lowest (Figs. 2C–E and 4C–E). Similarly, a decrease in chl_{DS} in slope waters of southern stations (MK $= -1.979$, $P = 0.048$, Supplementary Table 1) did not coincide with changes in phytoplankton size structure as inferred from $\gamma_{b_{bp}}$ (Fig. 2H).

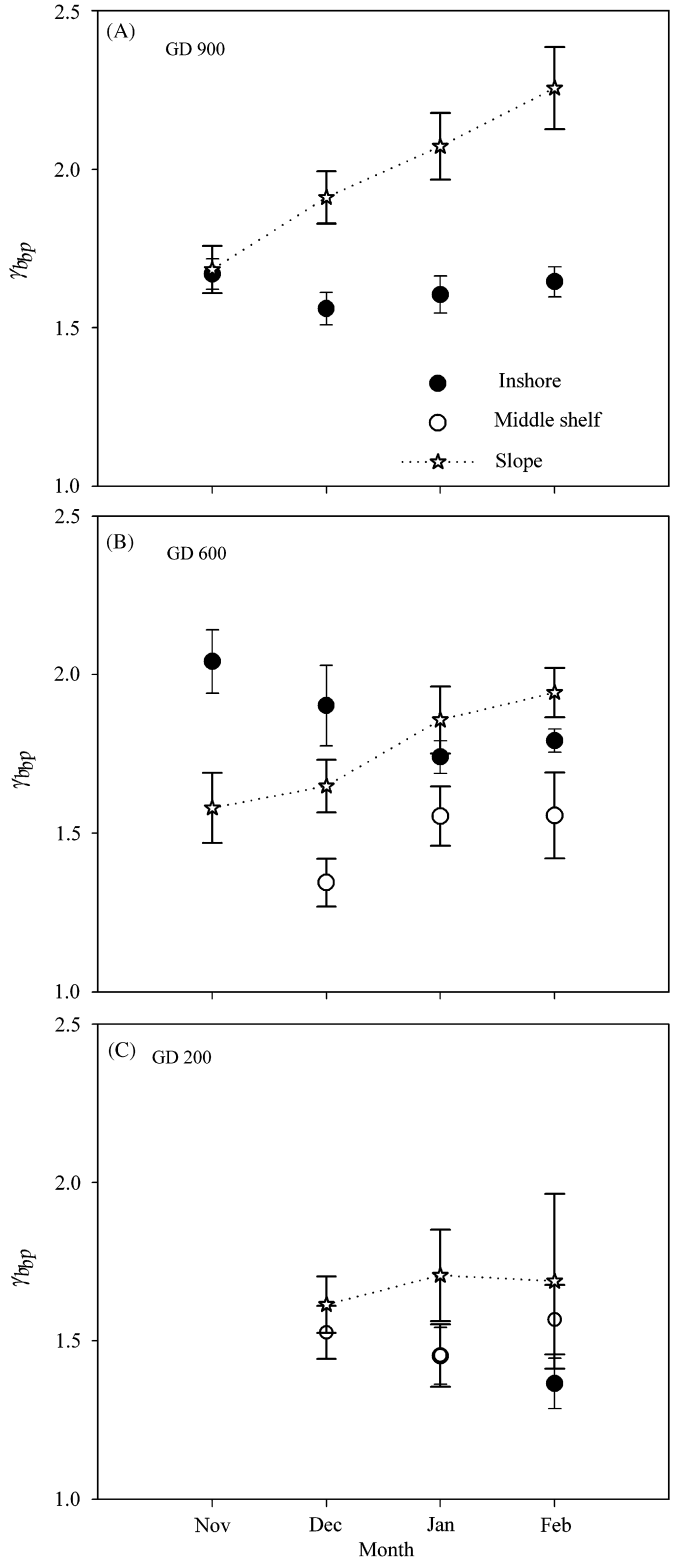

Fig. 3. Spring–summer variation of $\gamma_{b_{bp}}$ in the WAP region for 1997–2006. Monthly values of phytoplankton size structure index is depicted for inshore, middle shelf, and slope waters of WAP sampling; grid lines (GD) 900 (panel A), 600 (panel B), and 200 (panel C) correspond to northern, central and southern sampling stations. Middle shelf data of GD 900 are not plotted because this domain is occupied by Livingston Island. Lack of data during November is due mainly to the sea-ice cover (C) or proximity to Anvers Island (B).

3.3. Environmental variables

The seasonal sea-ice extent (monthly values) was inversely correlated with the inter-annual variability of $\gamma_{b_{bp}}$ (more sea ice, larger particles) in areas far from the coast and toward the North (lag $= -1$, R of Spearman up to -0.51 in slope waters of northern stations, Supplementary Table 3). Higher chl_{DS} values after a year with greater sea-ice extent was observed only for slope waters of northern stations (Spearman correlation $R = 0.41$, Supplementary Table 4, ftp://iod.ucsd.edu/mmontes). For 1997–2005, sea-ice extent in Bellingshausen Sea had a steady increase during December (Mann–Kendall test, MK $= 2.085$, $P = 0.037$, Supplementary Table 2). For a longer period of time (1978–2005), sea-ice extent decreases in this region between January and May (Mann–Kendall test, MK $= -2.603$, $P = 0.009$, Supplementary Table 1), confirming previous calculations (Smith and Stammerjohn, 2001). Additionally, sea-ice extent was inversely correlated with SAM and positively correlated with MEI values (see Supplementary Table 3). Positive and negative MEI values correspond with 'cold' (El Niño) and 'warm' (La Niña) ENSO events over the WAP region, respectively (Wolter and Timlin, 1998). Unlike WAP region, 'warming' phase in low-mid latitude environments is attributed to El Niño events. During SAM 'warm' phase (positive values), northerly winds blow over the WAP region (Stammerjohn et al., 2008). In some sub-regions of the WAP sampling grid (not northern stations), MEI anomalies varied in a positive way with $\gamma_{b_{bp}}$ values (Supplementary Table 3).

There was no evident correlation between inter-annual variability of SAM and phytoplankton size structure index values (see Supplementary Table 3). For WAP transects studied, the average water temperature for January 1997–2006 was not significantly different between regions across the shelf (Fig. 5, Table 1). In general, the range of water temperature was constrained over the survey area, with a large variability in southern (-0.48 to $2.2\,^{\circ}$C) and central (-1.22 to $2.2\,^{\circ}$C) stations. There was no clear correspondence between multi-annual variability of $\gamma_{b_{bp}}$ and sea-surface temperature (Figs. 2 and 5). Significant long-term decrease in water temperature in inshore, middle shelf and slope waters of southern stations (Supplementary Table 2) seemed not to have a remarkable effect on phytoplankton chlorophyll a fractions as derived from $\gamma_{b_{bp}}$ (Figs. 2G and 5A). Similar to water temperature, inter-annual variability in salinity values in central and southern transects was very irregular (Fig. 5C and D, $P > 0.05$). Significant decrease of salinity was detected in inshore and slope waters of GD 200 (Supplementary Table 2). As expected, the less salty waters (salinity ~33.5) were found in those areas highly influenced by sea ice (inshore of southern stations, Table 1, Fig. 5A). Variability of MLD between 1997 and 2005 did not have a clear association with $\gamma_{b_{bp}}$ variability in the region (Supplementary Table 1). A concomitant shallowing of MLD and reduction of mean cell size of phytoplankton (larger $\gamma_{b_{bp}}$) was only detected over the middle shelf of GD 600 (Spearman correlation, $R = -0.94$, Supplementary Table 3).

For all nutrients analyzed (macronutrients), there was no clear temporal trend (1997–2006) in each of the regions studied (Supplementary Table 1). Inter-annual variability of nutrient concentrations varied according to the type of nutrient and sampling site (Fig. 6). In general, we observed two types of temporal patterns: (1) irregular inter-annual variability, and (2) a cyclic pattern with a period of negative (nutrient depletion, 1997–2001) followed by a positive trend (nutrient enrichment, 2001–2005). The first temporal pattern was clearly seen at the southern stations, while the second temporal pattern appeared more evident at the central stations for all nutrients but NH_4^+. Roughly, these temporal patterns correlated negatively and

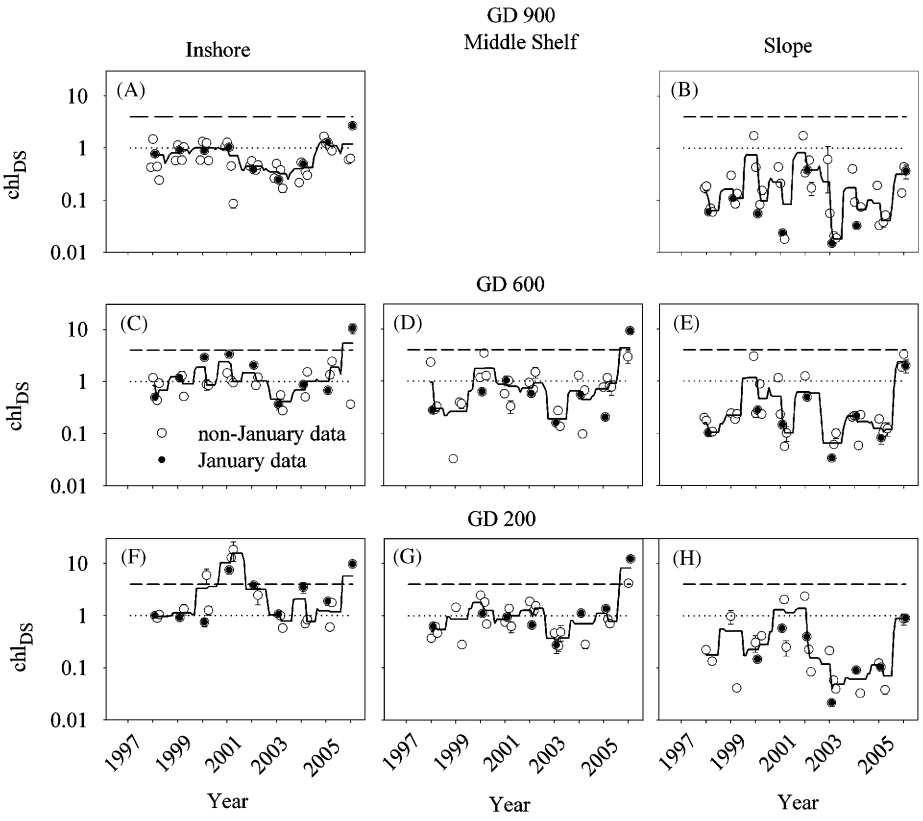

Fig. 4. Time series of satellite-derived chlorophyll *a* concentration (chl_{DS}) in the WAP region. For grid line (GD) 900 (northern transect, panels A and B), middle shelf data are not depicted because this domain is occupied by Livingston Island. GD 600 (panels C–E) and GD 200 (panels F–H) correspond to central and southern stations of WAP sampling grid, respectively. In log-scale, stations below dotted line and above dash line correspond to low ($<1\,mg\,m^{-3}$) and high ($>4\,mg\,m^{-3}$) phytoplankton biomass (Garibotti et al., 2003a), respectively. Each point in the graph represents a monthly average (November to February) 7 1 S.E. No monthly values are plotted when data are of poor quality or significantly affected by clouds or sea ice.

positively with chl_{DS} and $\gamma_{b_{bp}}$ at mid-shelf and inshore domains of northern stations, respectively (e.g., Figs. 2C and D, 4C–D and 6B, F and H). Spearman rank order comparisons evidenced a positive correlation between $\gamma_{b_{bp}}$ and NO_3^-+NO_2^- for slope waters of central and southern stations (Spearman correlation, $R = 0.81$–0.82, Supplementary Table 2). Significant R values also were calculated between $\gamma_{b_{bp}}$ and PO_4^{3-} for slope waters of central and southern stations, and inshore waters of southern stations.

4. Discussion

Motivated by the potential ecological consequences of regional climate change over WAP waters (Fraser and Patterson, 1997; Ducklow et al., 2007), this study explored the temporal and spatial variability in phytoplankton size structure in the region based on satellite and field observations (1997–2006). The size distribution of phytoplankton assemblages is a major biological factor that governs functioning of pelagic food-webs and consequently affects the rate of carbon export from the upper ocean to deep layers (Marañon et al., 2001). Likewise, the size spectrum of phytoplankton is very sensitive to long-term climate variability (Archer, 1995; Finkel et al., 2005). Therefore, phytoplankton size structure is a useful index to describe phytoplankton response and impact of that response on other ecosystem components to climate forcing. The interpretation of results is divided in two sections where spatial (4.1) and temporal variability (4.2) of phytoplankton size structure are analyzed as a function of environmental factors.

4.1. Spatial variations of phytoplankton size structure

Onshore–offshore gradients and latitudinal variations in phytoplankton size structure, as measured by the ($\gamma_{b_{bp}}$) index, had a fair correspondence with reported horizontal distributions of phytoplankton assemblages with different mean cell size and cell abundance. Likewise and based on $\gamma_{b_{bp}}$, west–east monthly differences on dominant phytoplankton size spectra were usually connected with sea-ice extent variability.

A common observation within transects analyzed (northern, central and southern stations) in the WAP was the increase in dominance of 'small' cells from onshore to offshore waters. This spatial pattern has been previously suggested for chlorophyll concentrations and net phytoplankton ($>20\,\mu m$) abundance (Smetacek et al., 1990; Baker et al., 1996; Bidigare et al., 1996; Garibotti et al., 2005b). However, on a finer scale, this was not always the case (e.g., middle shelf of central stations had a higher dominance of 'large' cells than inshore waters, Fig. 2C and D) supporting the idea of 'mosaics' of phytoplankton communities (Garibotti et al., 2005a). These complex spatial organizations have been attributed to year-to-year differences in phytoplankton seasonal succession from diatom to flagellates along the WAP sampling grid, presumably in response to variability in sea-ice retreat (Garibotti et al., 2003b).

Spectral changes on remote-sensing reflectance were also sensitive to along shelf differences in phytoplankton size structure as dominance of 'large' cells (lower $\gamma_{b_{bp}}$ values) increased from northern to southern stations of the WAP. Garibotti et al. (2003a) found that summer phytoplankton assemblages in the region

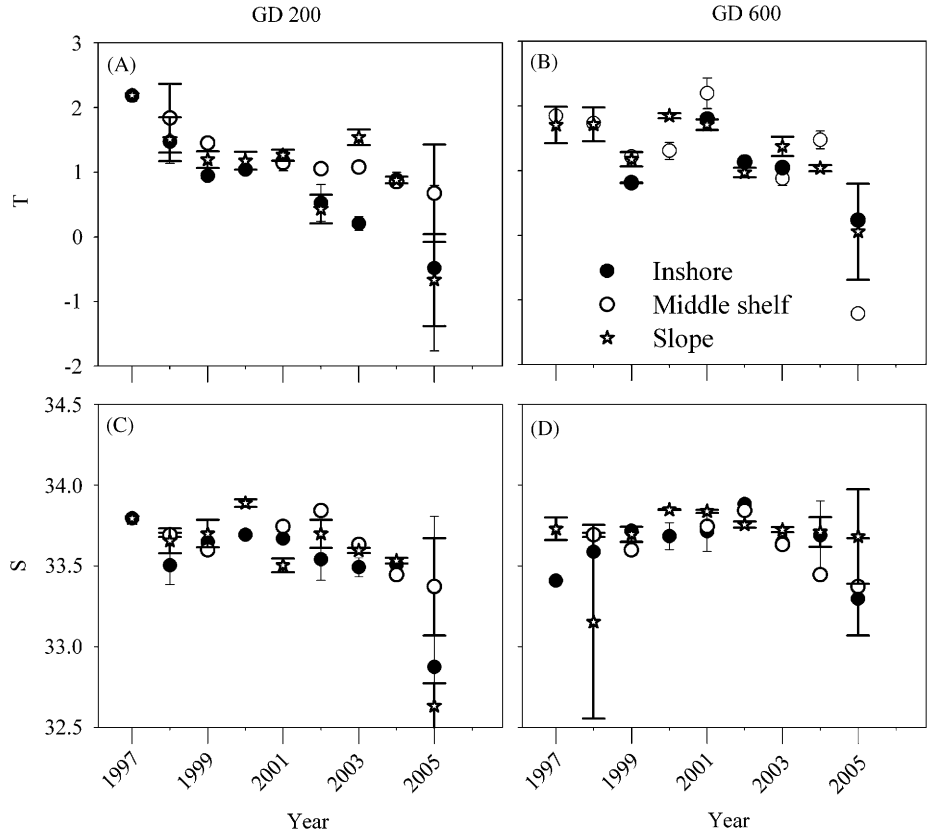

Fig. 5. Time series of surface-water temperature and salinity in the WAP region. No field data in northern stations (grid line or GD 900). GDs 600 and 200 correspond to central and southern stations of WAP sampling grid, respectively. *T* (panels A and B) and *S* (panels C and D) are the averaged surface temperature (°C) and salinity (non-dimensions). Each point in the graph represents a monthly average 7 1 S.E. (January, February) between 1997 and 2005.

(inshore and middle shelf) can be roughly divided into a northern (GD 600; defined as 'central' in this study) community of small-sized phytoplankton (cryptophytes) and a southern (GD 200) community of large-sized phytoplankton (diatoms). Likewise and supporting our index of phytoplankton size structure, the authors could not find latitudinal differences in phytoplankton composition of oceanic samples (slope domain). In the summer of 1997, four taxonomic clusters were defined based on microscopic identification between central and southern stations of the WAP sampling grid, three of which are present in our transects (Garibotti et al., 2003b, 2005b). The southernmost inshore stations in this study were located in waters adjacent to Marguerite Bay (Fig. 1) and were typically characterized by 'larger' cells. Inside Marguerite Bay, Garibotti et al. (2003b) defined a unique taxonomic consortium represented by large microphytoplankton diatoms (e.g., *Odontella weisflogii*), and a minor proportion of *P. antarctica*, and large prasinophytes (e.g., *Pyramimonas* sp.). Single cells of *P. antarctica* are considered nanoeukariotic algae (~5 μm) even though they can form colonies of up to 1 mm in response to environmental factors (e.g., zooplankton grazing; Lancelot et al., 1998). Thus, *P. antarctica* colonies may behave as 'large' phytoplankton cells, and may have been detected as larger particles by satellite observations (Montes-Hugo et al., 2008).

Consistent with dominance of 'small cells' in slope waters based on spectral changes, Garibotti et al. (2003b) defined a cluster with small-sized phytoplankton communities of oceanic and continental slope waters. These assemblages are dominated by nanoplanktonic (2–20 μm) diatoms (e.g., *Fragilariopsis curta*), which are expected to have low iron requirements compared to those of 'large' coastal species (Sunda and Huntsman, 1997; de Baar et al., 2005). In slope waters, the upper mixed layer is deeper than in middle shelf and inshore locations due to stronger winds and weaker stratification caused by sea-ice melting, thus greater light-iron co-limitation could be imposed onto 'large' diatoms (Hofmann et al., 2007).

Garibotti et al. (2003b) identified a cluster of mixed phytoplankton groups (unidentified flagellates, cryptophytes and prasinophytes) inhabiting mid-shelf and inshore waters of the northern and southern stations of the WAP sampling grid, excluding those in Marguerite Bay. In agreement with our cell size structure in central stations, this heterogeneous consortium, enriched in flagellate groups, was composed of cells larger and smaller than those in slope waters and Marguerite Bay, respectively.

The central–south gradients of 'large' (>20 μm) vs 'small' (<20 μm) phytoplankton assemblages might be explained by sea-ice dynamics. 'Large' phytoplankton species can be favored in adjacent waters to Marguerite Bay (inshore domain of southern stations) with respect to central stations because the greater sea ice persistence (percent time sea ice is present within the interval between day of advance and retreat) in this area (Tables 2 and 4 in Stammerjohn et al., 2008) which affect the timing of phytoplankton seasonal succession, as mentioned above. Sea ice may contribute also to the proportion of 'large' phytoplankton of surrounding waters by releasing 'large' cells stored during the previous winter. In artificial sea ice, Weissenberger and Grossmann (1998) commonly reported a greater incorporation of 'large' diatoms.

The selective sea-ice enhancement of 'large' with respect to 'small' phytoplankton cells associated with sea ice could be related in part to a greater availability of soluble iron. Iron-rich particles can be accumulated in sea ice as snow, and released to

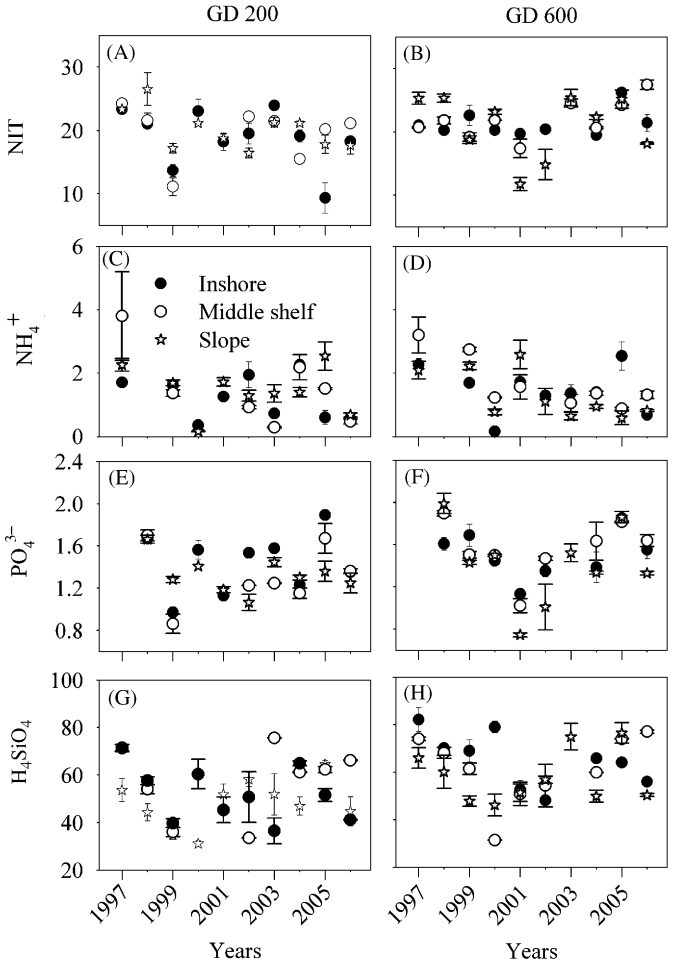

Fig. 6. Time series of surface nutrient concentrations in the WAP region. No field data in northern stations (grid line or GD 900). GDs 600 and 200 correspond to central and southern stations of WAP sampling grid, respectively. Nitrate+nitrite (NIT, panels A and B), ammonia (NH_4^+, panels C and D), phosphate (PO_4^{3-}, panels E and F), and silicic acid (H_4SiO_4, panels G and H) surface concentrations are in μM. Each point in the graph represents a monthly average 7 1 S.E. (January, February) between 1997 and 2006.

the ocean during sea ice melt (Measures and Vink, 2001). A comparable mechanism has been recently proposed for free-drifting icebergs. Smith et al. (2007) found that 'large-sized' diatoms cells are more abundant near (within 3.7 km) free-drifting icebergs, where concentration of dissolved iron is greater due to the transport of terrestrial iron-rich minerals (de Baar et al., 1995). A greater availability of iron in southern coastal waters of the WAP region due to the greater influence of sea ice might also explain the presence of *P. antarctica* in waters adjacent to Marguerite Bay. Sedwick et al. (2007) found that growth of *P. antarctica* in the Ross Sea is highly dependent on iron at relative low light intensities.

Differences on the depth of vertical mixing between central and south WAP stations also could explain the observed spatial patterns of phytoplankton size structure. Although some studies support the positive effect of water-column stratification on 'large' phytoplankton cells (Whitaker, 1982; Rivkin, 1991), this is not always the case (Hofmann et al., 2007). Deep vertical mixing may benefit smaller phytoplankton cells due to the greater iron limitation of larger phytoplankton cells at lower light intensities (light-iron co-limitation effect; Sunda and Huntsman, 1997; Timmermans et al., 2001). However, a shallower upper mixed layer does not necessary favor growth of all 'large' phytoplankton species (e.g., *Actinocylus* sp., *Chaetoceros dichaeta*) since high light levels can be inhibitory (Hofmann et al., 2007). The results from Spearman correlation did not show a clear relationship between 'large' phytoplankton cells (smaller $\gamma_{b_{bp}}$ values) and vertical mixing conditions (upper MLD) for southern stations (GD 200) of WAP where 'large' cells dominate (Supplementary Table 2).

The effect of zooplankton grazing on spatial patterns of phytoplankton size structure was not evaluated in this study but is expected to be secondary with respect to bottom-up effects over large areas of the Pal-LTER grid. In this region, grazing impact of dominant macro-zooplankton species (*Euphausia superba*, *Salpa thompsoni*) on phytoplankton is related to variations in grazer biomass (Ross et al., 1998). In terms of size, adults of *E. superba* have little direct utilization of nanophytoplankton compared to *S. thompsoni* (Quetin and Ross, 1985). Abundance of the two species is greatest in central stations (GD 600) (Ross et al., 2008) where phytoplankton size distribution is mainly characterized by small (high $\gamma_{b_{bp}}$) cells compared to southern stations. Likewise, onshore–offshore variations of *E. superba* and *S. thompsoni* densities coincide with the dominant phytoplankton size they use. Therefore, spatial modification of phytoplankton size structure due to macro-zooplankton grazing seems to be minor compared to other environmental factors.

4.2. Seasonal and inter-annual variability of phytoplankton size structure

In this study, time series of cell size distribution evidenced three main types of variability in phytoplankton size structure in the WAP: (1) year-to-year changes, (2) a multi-year sinusoidal pattern present in some sub-regions, and (3) trends in specific sub-regions.

Regarding year-to-year changes, Spearman correlation revealed that sea-ice extent may have a significant impact on inter-annual variations in phytoplankton size structure (Supplementary Table 2). As pointed out by Garibotti et al. (2005a), a delay in sea-ice retreat during spring might increase water-column stratification during the subsequent summer season, possibly affecting light and growth conditions for 'large' ($>20\,\mu m$) diatoms. The temporal sinusoidal pattern had two main features: (a) two maxima in spectral slope of particle backscattering (i.e. dominance of 'small' cells) during spring–summer of 1997–1998 and 2002–2003, where 'spring' is in October–November–December of 1997 and 2002, respectively (e.g., Fig. 2A, D, G, H), and (b) an inverse relationship between cell size structure and phytoplankton abundance (chl_{DS} concentration; e.g., Figs. 2 and 4A and H). On the basis of satellite measurements, Smith et al. (2008) observed that those chl_{DS} values over the WAP shelf and offshore of the shelf break (adjacent waters to the Southern Antarctic Circumpolar Current Front or SACCF) were anomalously low during summer of 1998 and 2003 with respect to the 1997–2005 mean. The authors found that a late sea-ice retreat offshore of the shelf break region and an early sea-ice retreat over the inshore shelf region occurred during the previous spring of 1997 and 2002. Stammerjohn et al. (2008) attribute this sub-regional variability in sea-ice retreat to the dynamic response of sea-ice extent to southerly winds. These sea-ice anomalies on offshore and inshore waters could explain the lack of offshore spring bloom and ice-edge bloom onto the shelf during January of 1998 and 2003, respectively. Since it is expected that phytoplankton blooms are characterized by 'large' cells (Smith and Nelson, 1990; Sullivan et al., 1993; Arrigo et al., 1999), we propose here that a larger contribution of 'small' ($<20\,\mu m$) phytoplankton cells during spring–summer of 1997–1998 and 2002–2003 can be attributed to drastic changes in sea-ice timing. Martinson et al. (2008) indicated that sea-ice seasons (first to first day of sea-ice

advance) 1997–1998 and 2002–2003 were also characterized by strong transitions in anomalies of ocean characteristics such as the increase on heat content of shelf waters (e.g., Upper Circumpolar Deep Water or UCDW intrusions). Along the shelf break of this region, there is an oceanic front (SACCF) defined by the southern boundary of the ACC (Orsi et al., 1995). The interaction between ACC and WAP shelf break causes surface entrainment of nutrient-rich and relatively warm waters from 200 to 800 m (UCDW) onto the shelf (Hofmann and Klinck, 1998; Smith et al., 1999). The intrusion over the WAP shelf is more significant in the southern part of the study area due to the well-developed across-shelf canyons (Martinson et al., 2008). Timing of sea-ice retreat and UCDW intrusions are consistent with large-scale changes in atmospheric conditions (e.g., wind intensity). Previous to 1998 and 2003 seasons, climate anomalies predominantly corresponded with a greater frequency of La Niña and SAM+ events, and a concomitant atmospheric and hydrographic warming over the WAP (Stammerjohn et al., 2008). Although the maxima in 1998 and 2003 corresponding to dominance of 'small' cells were detected in regions close (inshore) or far (slope) from the coast, and at the North (northern) or South (southern WAP stations) of the study area (Fig. 2A and H), this temporal pattern could not be generalized over the whole study area. This finding is not surprising given the unique oceanographic and climate characteristics of each sub-region (e.g., the northernmost transect is more influenced by glacial meltwater than the southernmost transect; Stammerjohn et al., 2008). The contribution of macrozooplankton grazing to the observed cyclic pattern of phytoplankton cell size dominance is unclear. However, it might be expected a greater direct influence of short-life (*S. thompsoni*, 1–2 years) compared to long-life (*E. superba*, 4–6 years) species. Although *S. thompsoni* has been more frequently found across the WAP shelf from 1999 to the present (Ross et al., 2008), this evidence does not appear to indicate a sustained increase of phytoplankton cell size (small $\gamma_{b_{bp}}$) over the same locations and period of time. Perhaps the main influence of *S. thompsoni* is indirect, as salps also feed on microzooplankton (protozoa), favoring growth of 'small' phytoplankton species. Variation of concentration of macronutrients was not the cause of observed cyclic pattern of phytoplankton size structure in WAP waters because two reasons. First, the 'V' temporal variation of all nutrients but NH_4^+ between 1997 and 2006 was not evident in GD 200, where $\gamma_{b_{bp}}$ presented a clear 'V'-type temporal fluctuation had. Second, dominance of smaller phytoplankton cells is expected in nutrient-poor waters, but highest $\gamma_{b_{bp}}$ values (small cells) were observed during periods of high nutrient concentrations (summer of 1998 and 2003).

Detectable trends over the time period studied (1997–2006) was the third type of pattern in temporal variability in phytoplankton size structure in the WAP. The observed trends had two main characteristics: (1) a net change superimposed to the seasonal variability in particle size distribution and (2) a positive or negative sign (e.g., positive MK corresponds to an increase in particle size distribution) depending on location. On the basis of Mann–Kendall analysis, dominance of particle size distributions with smaller particles (smaller phytoplankton cells, higher $\gamma_{b_{bp}}$ values) increased significantly from 1997 to 2006 in inshore waters of northern stations (GD 900). Unfortunately, no field data is available to corroborate this finding. The observed trend might be caused by increased local glacial-ice melting (e.g., more contribution of small cryptophytes as proposed by Moline et al., 2004), elevated grazing of adult krill and large copepods (e.g., less contribution of microphytoplankton; Bianchi et al., 1992; Rodriguez et al., 2002), or/and a stronger advection of waters 'rich' in 'small' cells (e.g., nanoflagellates less than 20 μm; Bianchi et al., 1992; Granéli et al., 1993; Krell et al., 2005) from Weddell Sea into the eastern part of the Bransfield Strait (Hofmann et al., 1996; Zhou et al., 2002).

According to Mann–Kendall results, a significant trend was detected in slope waters of central stations of the WAP sampling grid (GD 600) where contribution of larger phytoplankton (smaller $\gamma_{b_{bp}}$ values) augmented from 1997 to 2006. This phenomenon might be related to a greater growth of diatoms compared to small phytoflagellates favored by stronger upwelling events (Prézelin et al., 2000). During January 1993, diatom-dominated assemblages were associated with a topographically induced upwelling along the outer WAP continental shelf. These waters were characterized at depth (250 m) by temperature values (1.8 °C), indicative of UCDW flowing onto the shelf. Diatom communities can meet nutrient growth requirements in these areas due to the greater availability of silicate (Prézelin et al., 2000) or iron (Garibotti et al., 2003b). Although silicate is assumed not to be a limiting nutrient south of the Antarctic Polar Front (Hofmann et al., 2007), active phytoplankton growth nearby topographically induced upwelling centers might require a surplus of this nutrient. The increase of phytoplankton cell size in these topographically induced upwelling zones also could be explained by an enhanced of microzooplankton grazing (e.g., smaller phytoplankton is consumed) even though no data are available to test this possibility.

5. Conclusions

High-latitude marine environments are expected to be sensitive ecosystems to climate change due to their dependence on sea ice. One of the best examples is the WAP region where one of the fastest atmospheric warming and decrease in sea-ice extension and length of the sea-ice season have been detected in the last five decades (Smith and Stammerjohn, 2001; Martinson et al., 2008). In this study, potential climate modifications of lower trophic levels between 1997 and 2006 were investigated in the WAP region based on variability of phytoplankton size structure, a well-known index of trophic dynamics in pelagic waters. Satellite and complimentary field information revealed three types of temporal patterns: (1) inter-annual variability, (2) transitional periods caused by regime shift, and (3) 9-year trends. The series analyzed is too short to give answers to the response of phytoplankton to the 50-year climate trend in atmospheric temperature. Nevertheless, we have demonstrated that phytoplankton size structure, as measured by remote sensing, is a valid index of variability in ecosystem structure and we have established the main patterns of variability that can be expected to be affected by climate change. We also suggest that bottom-up (e.g., sea-ice dynamics) effects can have a significant spatial and temporal influence on phytoplankton size structure variability of WAP study area. Despite the decrease of sea-ice coverage and general atmospheric warming of WAP waters, our findings based on a 'time window' of circa 10-years do not indicate an overall replacement of phytoplankton from communities dominated by 'large' cells to communities dominated by 'small' cells during spring–summer of 1997–2006. Therefore, the original hypothesis that 'contribution of "small" phytoplankton (<20 μm) has been increased in the last decade in WAP waters due the ongoing regional climate change' cannot be accepted. Although a significant cell size reduction of phytoplankton assemblages was detected in the northernmost part of the area investigated, an opposite trend was found for phytoplankton communities living in slope waters of central stations. Therefore, it appears that there is not a general regional response of phytoplankton size structure to the increasing warming of WAP shelf waters. Instead, the climate variability over WAP seems to affect differently the size distribution of

phytoplankton depending on the latitude and the distance to the coast. As a greater frequency of anomalous wind episodes (e.g., southerlies) may favor dominance of 'small' phytoplankton communities, a greater intensification of ACC interaction with the WAP shelf-break can result in a greater dominance of 'large' phytoplankton communities.

Acknowledgments

We thank to the people that collected and processed the field data, Karen Baker, Janice Jones, Wendy Kozlowski, and Karie Sines. Also, we appreciated all logistic assistance given by the RV Polar Duke and ARV L.M. Gould crew members. This work was supported by Palmer NSF Grant OPP-02-17282. We thank the constructive comments of anonymous reviewers. This is the LTER contribution] 0297.

References

Archer, D., 1995. Upper ocean physics as relevant to ecosystem dynamics: a tutorial. Ecological Applications 5, 724–739.

Arrigo, K.R., Robinson, D.H., Worthen, D.L., Dunbar, R.B., DiTullio, G.R., VanWoert, M., Lizotte, M.P., 1999. Phytoplankton community structure and the drawdown of nutrients and CO_2 in the Southern Ocean. Science 283, 365–367.

Baker, K.S., Vernet, M., Fraser, W.R., Trivelpiece, W.Z., Hofmann, E.E., Klinck, J.M., Karl, D.M., Quetin, L.B., Ross, R.M., Smith, R.C., 1996. The western Antarctic Peninsula region: summary of environmental and ecological processes. In: Ross, R.M., Hofmann, E.E., Quetin, L.B. (Eds.), Foundations for Ecological Research West of the Antarctic Peninsula. Antarctic Research Series 70. American Geophysical Union, Washington, pp. 437–448.

Bianchi, F., Boldrin, A., Cioce, F., Dieckmann, G., Kuosa, H., Larsson, A.M., Nöthig, E.M., Sehlsedt, P.I., Socal, G., Syvertsen, E.E., 1992. Phytoplankton distribution in relation to sea ice, hydrography and nutrients in the northwestern Weddell Sea in early spring 1988 during EPOS. Polar Biology 12, 225–235.

Bidigare, R.R., Iriarte, J.L., Khan, S.H., Karentz, D., Ondrusek, M.E., Fryxell, G.A., 1996. Phytoplankton: qualitative and quantitative assessments. In: Ross, R., Hoffmann, E., Quetin, L. (Eds.), Foundations for Ecosystem Research in the western Antarctic Peninsula Region. American Geophysical Union, Washington, DC, pp. 173–198.

Carder, K.L., Chen, F.R., Lee, Z.P., Hawes, S.K., 1999. Semianalytical moderate-resolution imaging spectrometer algorithms for chlorophyll a and absorption with bio-optical domains based on nitrate-depletion temperatures. Journal of Geophysical Research 104 (c3), 5403–5421.

Carder, K.L., Chen, F.R., Cannizzaro, J.P., Campbell, J.W., Mitchell, B.G., 2004. Performance of the MODIS semi-analytical ocean color algorithm for chlorophyll-*a*. Advances in Space Research 33, 1152–1159.

Caron, D.A., Dennett, M.R., Lonsdale, D.J., Moran, D.M., Shalapyonok, L., 2000. Microzooplankton herbivory in the Ross Sea Antarctica. Deep-Sea Research II 47, 3249–3272.

Comiso, J.C., 1995. Sea-ice geophysical parameters from SMMR and SSM/I data. In: Ikeda, M., Dobson, F. (Eds.), Oceanographic Applications of Remote Sensing. CRC Press, Boca Raton, FL, pp. 321–338.

Comiso, J.C., Cavalieri, D., Parkinson, C., Gloersen, P., 1997. Passive microwave algorithms for sea-ice concentration—a comparison of two techniques. Remote Sensing of Environment 60, 357–384.

De Baar, H.J.W., de Jong, J.T.M., Bakker, D.C.E., Löscher, B.M., Veth, C., Bathmann, U., Smetacek, V., 1995. Importance of iron for phytoplankton spring blooms and CO_2 drawdown in the Southern Ocean. Nature 373, 412–415.

De Baar, H.J.W., Van Leeuwe, M.A., Scharek, R., Goeyens, L., Bakker, K.M.J., Fritsche, P., 1997. Nutrient anomalies in Fragilariopsis kerguelensis blooms, iron deficiency and the nitrate/phosphate ratio (A.C. Redfield) of the Antarctic Ocean. Deep-Sea Research II 44, 229–260.

De Baar, H.J.W., Boyd, P.W., Coale, K.H., et al., 2005. Synthesis of iron fertilization experiments: from the iron age of enlightment. Journal of Geophysical Research 110 (c09), s16.

Dierssen, H.M., Smith, R.C., 2000. Bio-optical properties and remote sensing ocean color algorithms for Antarctic Peninsula waters. Journal of Geophysical Research 105 (26), 26,301–26,312.

Ducklow, H.W., Baker, K., Martinson, D.G., Quetin, L.B., Ross, R.M., Smith, R.C., Stammerjohn, S.E., Vernet, M., Fraser, W., 2007. Marine pelagic ecosystems: the West Antarctic Peninsula. Philosophical Transactions of the Royal Society of London B Biological Sciences 362, 67–94.

Finkel, Z.V., Katz, M.E., Wright, J.D., Schofield, O.M., Falkowski, P., 2005. Climatically driven macroevolutionary patterns in the size of marine diatoms over the Cenozoic. Proceedings of the National Academy of Sciences of the United States of America 102, 8927–8932.

Fraser, W.R., Patterson, D.L., 1997. Human disturbance and long-term changes in Adelie penguin populations: a natural experiment at Palmer Station, Antarctica Peninsula. In: Battaglia, B., Valencia, J., Walton, D.W.H. (Eds.), Antarctic Communities: Species, Structure and Survival. Cambridge University, Press, Cambridge, pp. 445–452.

Garibotti, I.A., Vernet, M., Ferrario, M.E., Smith, R.C., Ross, R., Quetin, L.B., 2003a. Phytoplankton spatial distribution patterns along the western Antarctic Peninsula (Southern Ocean). Marine Ecology Progress Series 261, 21–39.

Garibotti, I., Vernet, M., Kozlowski, W.A., Ferrario, M.E., 2003b. Composition and biomass of phytoplankton assemblages in coastal Antarctic waters: a comparison of chemotaxonomic and microscopic analyses. Marine Ecology Progress Series 247, 27–42.

Garibotti, I.A., Vernet, M., Ferrario, M.E., 2005a. Annually recurrent phytoplanktonic assemblages during summer in the seasonal ice zone west of the Antarctic Peninsula (Southern Ocean). Deep-Sea Research I 52, 1823–1841.

Garibotti, I.A., Vernet, M., Smith, R.C., Ferrario, M., 2005b. Interannual variability in the distribution of the phytoplankton standing stock across the seasonal sea-ice zone west of the Antarctica Peninsula. Journal of Plankton Research 27, 825–843.

Gordon, H.R., Morel, A., 1983. Remote Assessment of Ocean Color for Interpretation of Satellite Visible Imagery: A Review. Springer, New York.

Gordon, H.R., Brown, J.W., Brown, O.B., Evans, R.H., Clark, D.K., 1988. Exact Rayleigh scattering calculations for use with the Nimbus-7 coastal zone color scanner. Applied Optics 27, 862–871.

Granéli, E., Granéli, W., Mozzam Rabbani, M., Daugbjerg, N., Fransz, G., Cuzin-Roudy, J., Alder, V., 1993. The influence of copepod and krill grazing on the species composition of phytoplankton communities from the Scotia-Weddell Sea: an experimental approach. Polar Biology 13, 201–213.

Hirsch, R.M., Slack, J.R., Smith, R.A., 1982. Techniques of trend analysis for monthly water quality data. Water Resources Research 18, 107–121.

Hofmann, E.E., Klinck, J.M., 1998. Thermohaline variability of the waters overlying the West Antarctic Peninsula continental shelf, ocean, ice, atmosphere. In: Jacobs, S., Weiss, R. (Eds.), Interactions at the Antarctic Continental Margin. American Geophysical Union, Antarctic Research Series, vol. 75, pp. 67–81.

Hofmann, E.E., Klinck, J.M., Lascara, C.M., Smith, D.A., 1996. Water mass distribution and circulation west of the Antarctic Peninusla and including Bransfield Strait. In: Ross, R.M., Hofmann, E.E., Quetin, L.B. (Eds.), Foundations for Ecological Research West of the Antarctic Peninsula. American Geophysical Union, Washington, pp. 61–80.

Hofmann, L.J., Peeken, I., Lochte, K., 2007. Co-limitation by iron, silicate, and light of three Southern Ocean diatom species. Biogeosciences Discussions 4, 209–247.

Holm-Hansen, O., Mitchell, B.G., Hewes, C.D., Karl, D.M., 1989. Phytoplankton blooms in the vicinity of palmer station, Antarctica. Polar Biology 10, 49–57.

Johnson, K.S., Petty, R.L., Thomsen, J., 1985. Continuous flow injection for seawater micronutrients. In: Zirino, A. (Ed.), Mapping Strategies in Chemical Oceanography. Advances in Chemistry Series, vol. 209. American Chemical Society, pp. 7–30.

Kendall, M.G., 1975. Rank Correlation Methods, fourth ed. Charles Griffin, London.

Krell, A., Schnack-Schiel, S.B., Thomas, D.N., Katner, G., Zipan, W., Dieckmann, G.S., 2005. Phytoplankton dynamics in relation to hydrography, nutrients and zooplankton at the onset of sea ice formation in the eastern Weddell Sea (Antarctica). Polar Biology 28, 700–713.

Kwok, R., Comiso, J.C., 2002. Southern Ocean climate and sea ice anomalies associated with the Southern Oscillation. Journal of Climate 15, 487–501.

Lancelot, C., Keller, M.D., Rousseau, V., Smith, W.O., Mathot, S., 1998. Autoecology of the marine haptophyte Phaeocystis sp. In: Anderson, D.M., Cembelia, A.D., Hallagraeff, G.M. (Eds.), Physiological Ecology of Harmful Algal Blooms. Springer, Berlin, pp. 209–224.

Landry, M., Brown, S.L., Selph, K.E., Abbott, M.R., Letelier, M.R., Christensen, S., Bidigare, R.R., Casciotti, K., 2001. Initiation of the spring phytoplankton increase in the Antarctic Polar Front Zone at 170°W. Journal of Geophysical Research 106 (C7), 13903–13916.

Libiseller, C., Grimvall, A., 2002. Performance of partial Mann Kendall tests for trend detection in the presence of covariates. Environmetrics 13, 71–84.

Liu, J., Curry, J.A., Martinson, D.G., 2004. Interpretation of recent Antarctic sea ice variability. Geophysical Research Letters 31 (L02205), 1–4.

Loeb, V., Siegel, V., Holm-Hansen, O., et al., 1997. Effects of sea-ice extent and krill or salp dominance on the Antarctic food web. Nature 387, 897–900.

Mann, H.B., 1945. Nonparametric tests against trend. Econometrica 13, 245–259.

Marañon, E., Holligan, P.M., Barciela, R., González, N., Mouriño, B., Pazó, M.J., Varela, M., 2001. Patterns of phytoplankton size–structure and productivity in contrasting open ocean environments. Marine Ecology Progress Series 216, 43–56.

Marshall, G.J., 2003. Trends in the Southern Annular Mode from observations and reanalyses. Journal of Climatology 14, 4134–4143.

Martinson, D., Iannuzzi, R.A., 1998. Antarctic ocean-ice interactions: implications from ocean bulk property distributions in the Weddell gyre. In: Jeffries, M.O. (Ed.), Antarctic Sea Ice: Physical Processes, Interactions and Variability. Antarctic Research Series, vol. 74, American Geophysical Union, pp. 243–271.

Martinson, D.G., Iannuzzi, R., Allspaw, S., 1999. CTD operations manual—RV1B Nathaniel B. Palmer. Antarctic Support, Associates Technical Report.

Martinson, D.G., Stammerjohn, S.E., Iannuzzi, R.A., Smith, R.C., Vernet, M., 2008. Western Antarctic Peninsula physical oceanography and spatio–temporal variability. Deep-Sea Research II, this issue [doi:10.1016/j.dsr2.2008.04.038].

Measures, C.I., Vink, S., 2001. Dissolved Fe in the upper waters of the Pacific sector of the Southern Ocean. Deep-Sea Research II 48, 3913–3941.

Moline, M.A., Prézelin, B.B., 1996. Palmer LTER 1991–1994: long-term monitoring and analyses of physical factors regulating variability in coastal Antarctic phytoplankton biomass, in situ productivity and taxonomic composition over

subseasonal, seasonal, and interannual time scales phytoplankton dynamics. Marine Ecology Progress Series 145, 143–160.
Moline, M.A., Prézelin, B.B., Schofield, O., 1997. Palmer-LTER: stable inter-annual successional patterns of phytoplankton communities in the coastal waters off Palmer Station, Antarctica. Antarctic Journal, 151–153.
Moline, M.A., Claustre, H., Fraser, T.K., Schofield, O., Vernet, M., 2004. Alteration of the food web along the Antarctic Peninsula in response to a regional warming trend. Global Change Biology 10, 1973–1980.
Montes-Hugo, M., Carder, K., Foy, R., Cannizzaro, J., Brown, E., Pegau, S., 2005. Estimating phytoplankton biomass in coastal waters of Alaska using airborne remote sensing. Remote Sensing of Environment 98, 481–493.
Montes-Hugo, M., Vernet, M., Smith, R., Carder, K., 2008. Phytoplankton size structure on the Western shelf of the Antarctic Peninsula: a remote sensing approach. International Journal of Remote Sensing 29, 801–829.
O'Reilly, J.E., Maritorena, S., Mitchell, B.G., Siegel, D.A., Carder, K., Garver, S.A., Karhu, M., McClain, C.R., 1998. Ocean color algorithms for SeaWiFS. Journal of Geophysical Research 103 (c11), 24937–24953.
Orsi, A.H., Withworth, T., Nowlin, W.D., 1995. On the meridional extent and fronts of the Antarctic Circumpolar Current. Deep-Sea Research I 42, 641–673.
Perissinotto, R., Pakhomov, E.A., 1998. Contribution of salps to carbon flux of marginal ice zone of the Lazarev Sea, Southern Ocean. Marine Biology 131, 25–32.
Prézelin, B.B., Hofmann, E.E., Mengelt, C., Klinck, J.M., 2000. The linkage between Upper Circumpolar Deep Water (UCDW) and phytoplankton assemblages on the west Antarctic Peninsula continental shelf. Journal of Marine Research 58, 165–202.
Prézelin, B.B., Hoffmann, E.E., Moline, E., Klinck, J.M., 2004. Physical forcing of phytoplankton community structure and primary production in continental shelf waters of the western Antarctic Peninsula. Journal of Marine Systems 62, 419–460.
Quetin, L.B., Ross, R.M., 1985. Feeding by Antarctic krill, *Euphausia superba*: does size matter? In: Siegfried, W.R., Condy, P.R., Laws, R.M. (Eds.), Antarctic Nutrient Cycles and Food Webs. Springer, Berlin, pp. 372–377.
Rivkin, R.B., 1991. Seasonal patterns of planktonic production in McMurdo Sound, Antarctica. American Zoology 31, 5–16.
Rodriguez, J., Jiménez-Gómez, F., Blanco, J.M., Figueroa, F.L., 2002. Physical gradients and spatial variability of the size structure and composition of phytoplankton in the Gerlache Strait (Antarctica). Deep-Sea Research II 49, 693–706.
Ross, R.M., Quetin, L.B., Haberman, K.L., 1998. Interannual and seasonal variability in short-term grazing impact of *Euphausia superba* in nearshore and offshore waters west of the Antarctic Peninsula. Journal of Marine Systems 17 (1–4), 261–273.
Ross, R.M., Quetin, L.B., Martinson, D.G., Iannuzzi, R., Stammerjohn, S., Smith, R.C., 2008. Palmer LTER: patterns of distribution of five dominant zooplankton species in the epipelagic zone west of the Antarctic Peninsula (1993–2004). Deep-Sea Research II 55, 2086–2105.
Sedwick, P.N., Garcia, N.S., Riseman, S.F., Marsay, C.M., DiTullio, G.R., 2007. Evidence of high iron requirements of colonial *Phaeocystis antarctica* at low irradiance. Biogeochemistry 83, 83–97.
Simmonds, I., King, J.C., 2004. Global and hemispheric climate variations affecting the Southern Ocean. Antarctic Science 16, 401–413.
Smetacek, V., Scharek, R., Nöthig, E.M., 1990. Seasonal and regional variation in the pelagial and its relationship to the life history cycle of krill. In: Kerry, K.R., Hempel, G. (Eds.), Antarctic Ecosystems, Ecological Change and Conservation. Springer, Berlin, pp. 103–114.
Smith Jr., W.O., Nelson, D.M., 1990. Phytoplankton growth and new production in the Weddell Sea marginal ice zone in the austral and spring and autumn. Limnology and Oceanography 35, 809–821.
Smith, R.C., Stammerjohn, S.E., 2001. Variations of surface air temperature and sea ice extent in the western Antarctic Peninsula (WAP) region. Annals of Glaciology 33, 493–500.
Smith, R.C., Stammerjohn, S.E., 2003. An LTER network overview and introduction of El Nino-Southern Oscillation (ENSO) climatic signal and response, Chapter II, pp. 102–117. In: Greenland, D., Goodin, D.G., Smith, R. (Eds.). Climate Variability and Ecosystem Response at Long-Term Ecological Research Sites, Long-Term Ecological Research Network Series. Oxford University Press, 480pp.
Smith, W.O., Lancelot, C., 2004. Bottom-up versus top-down control in phytoplankton of the Southern Ocean. Antarctic Science 16, 531–539.
Smith, R.C., Baker, K.S., Dustan, P., 1981. Fluorometric techniques for the measurement of oceanic chlorophyll in the support of remote sensing. Scripps Institution of Oceanography, University of California (Refs. 81–17).
Smith, R.C., Baker, K.S., Fraser, W.R., Hofmann, E.E., Karl, D.M., Klinck, J.M., Quetin, L.B., Prézelin, B.B., Ross, R.M., Trivelpiece, W.Z., Vernet, M., 1995. The Palmer LTER: a long-term ecological research program at Palmer Station, Antarctica. Oceanography 8, 77–86.
Smith, R.C., Menzies, D.W., Booth, C.R., 1997. Oceanographic biooptical profiling system II. Proceedings of the PIE International Society of Optical Engineering 2963, 777–786.
Smith, D.A., Hofmann, E.E., Klinck, J.K., Lascara, C.M., 1999. Hydrography and circulation in the west Antarctic Peninsula continental shelf. Deep-Sea Research I 46, 951–984.
Smith Jr., K., Robison, B.H., Helly, J.J., Kaufmann, R.S., Ruhl, H.A., Shaw, T.J., Twining, B.S., Vernet, M., 2007. Free-drifting icebergs: hot spots of chemical and biological enrichment in the Weddell Sea. Science 10, 1126.
Smith, R.C., Martinson, D.G., Stammerjohn, S.E., Iannuzzi, R., Ireson, K., 2008. Bellingshausen and western Antarctic Peninsula region: pigment biomass and sea ice spatial/temporal distributions and inter-annual variability. Deep-Sea Research II 55, 1949–1963.
Sokal, R.R., Rohlf, F.J., 1995. Biometry. W.H. Freeman & Company, New York, 498pp.
Sprules, W.G., Munawar, M., 1986. Plankton size spectra in relation to ecosystem productivity, size, and perturbation. Canadian Journal of Fisheries and Aquatic Sciences 43, 1789–1794.
Stammerjohn, S.E., Drinkwater, M.R., Smith, R.C., Liu, X., 2003. Ice-atmosphere interactions during sea-ice advance and retreat in the western Antarctic Peninsula region. Journal of Geophysical Research 108 (c10), 1–15.
Stammerjohn, S.E., Martinson, D.G., Smith, R.C., Ianuzzi, R.A., 2008. Sea ice in the Western Antarctic Peninsula region: spatio-temporal variability from ecological and climate change perspectives. Deep-Sea Research II 55, 2041–2058.
Sullivan, C.W., Arrigo, K.R., McClain, C.R., Comiso, J.C., Firestone, J., 1993. Distributions of phytoplankton blooms in the Southern Ocean. Science 262, 1832–1837.
Sunda, W.G., Huntsman, S.A., 1997. Interrelated influence of iron, light and cell size on marine phytoplankton growth. Nature 390, 389–392.
Timmermans, K.R., Davey, M.S., van der Wagt, B., 2001. Co-limitation by iron and light of *Chaetoceros brevis*, *C. dichaeta*, *C. calcitrans* (Bacillariophyceae). Marine Ecology Progress Series 217, 287–297.
Varela, M., Fernández, E., Serret, P., 2002. Size-fractionated phytoplankton biomass and primary production in the Gerlache and Bransfield straits (Antarctic Peninsula) in the Austral summer 1995–1996. Deep-Sea Research II 49, 749–768.
Walsh, J.J., Dieterle, D.A., Lenes, J., 2001. A numerical analysis of carbon dynamics of the Southern Ocean phytoplankton community: the roles of light and grazing in effecting both sequestration of atmospheric CO_2 and food availability to larval krill. Deep-Sea Research Part I 48, 1–48.
Waters, K., Smith, R.C., 1992. Palmer LTER: a sampling grid for the Palmer LTER program. Antarctic Journal of United States 236, 237.
Weissenberger, J., Grossmann, S., 1998. Experimental formation of sea ice: importance of water circulation and wave action for incorporation of phytoplankton and bacteria. Polar Biology 20, 178–188.
Whitaker, T.M., 1982. Primary production of phytoplankton off Signy Island, South Orkneys, The Antarctic. Proceedings of the Royal Society London, Series B 214, 169–189.
Wolter, K., Timlin, M.S., 1998. Measuring the strength of ENSO—how does 1997/98 rank? Weather 53, 315–324.
Zhou, M., Niiler, P.P., Hu, J.H., 2002. Surface currents in the Bransfield and Gerlache Straits, Antarctica. Deep-Sea Research I 49, 267–280.